

A Novel Prediction Model Based on Quantitative Texture Analysis of Sonographic Images for Malignant Major Salivary Glandular Tumors

CME Credits

Wu-Chia Lo^{1,2,3}, Ping-Chia Cheng^{1,2,4}, Wan-Lun Hsu⁵, Po-Wen Cheng¹, Li-Jen Liao^{1,2,6,7*}

¹Department of Otolaryngology Head and Neck Surgery, Far Eastern Memorial Hospital, New Taipei, Taiwan, ²Head and Neck Cancer Surveillance and Research Study Group, Far Eastern Memorial Hospital, New Taipei City, Taiwan, ³Graduate Institute of Medicine, Yuan Ze University, Taoyuan, Taiwan, ⁴Department of Communication Engineering, Asia Eastern University of Science and Technology, New Taipei, Taiwan, ⁵Genomics Research Center, Academia Sinica, Taipei, Taiwan, ⁶Department of Electrical Engineering, Yuan Ze University, Taoyuan, Taiwan, ⁷Biomedical Engineering Office, Far Eastern Memorial Hospital, Taipei, Taiwan

Abstract

Background: The aim of this study was to compare multiple objective ultrasound (US) texture features and develop an objective predictive model for predicting malignant major salivary glandular tumors. **Methods:** From August 2007 to May 2018, 144 adult patients who had major salivary gland tumors and subsequently underwent surgery were recruited for this study. Representative brightness mode US pictures were selected for texture analysis and used to develop a prediction model. **Results:** We found that the grayscale intensity and standard deviation of the intensity were significantly different between malignant and pleomorphic adenomas. The contrast, inverse difference (INV) movement, entropy, dissimilarity, and INV also differed significantly between benign and malignant tumors. We used stepwise selection of predictors to develop an objective predictive model, as follows: $\text{Score} = 1.138 \times \text{Age} - 1.814 \times \text{Intensity} + 1.416 \times \text{Entropy} + 1.714 \times \text{Contrast}$. With an optimal cutoff of 0.58, the diagnostic performance of this model had a sensitivity, specificity, overall accuracy, and area under the curve of 83% (95% confidence interval [CI]: 74%–92%), 74% (65%–84%), 78% (72%–85%), and 0.86 (0.80–0.92), respectively. **Conclusion:** We have developed a novel computerized diagnostic model based on objective US features to predict malignant major salivary gland tumor. Further improving the computer-aided diagnosis model might change the US examination for major salivary gland tumors in the future.

Keywords: Prediction model, salivary gland tumors, texture, ultrasound

INTRODUCTION

Major salivary glands include the parotid, submandibular, and sublingual glands. Imaging modalities are useful in the contemporary evaluation of salivary gland disorders. Ultrasound (US) can readily assess the major salivary glands and may obviate the need for further imaging and provide a reliable estimation of tumor location.^[1] Under US examination, the normal major salivary glands are homogeneous echogenic organs.^[2] Although the US is sensitive for detecting salivary glandular tumors, its specificity in the differentiation of these tumors is limited by individual characteristics. Besides, US is technique and operator dependent; it is also difficult in evaluating deep lobe parotid tumors, and no single feature is sufficient to differentiate benign from malignant salivary gland tumor. Previously, we combined multiple characteristics

to develop a predictive model for malignant salivary gland tumors,^[3] though reliance on human expertise remains. Developing an objective sonographic predictive model may be helpful for diagnosing malignant major salivary glandular tumors and avoiding operator subjective judgment.

Image texture analysis is a novel method to analyze imaging objectively.^[4] First-order quantitative analysis uses an image histogram to calculate texture. It has been used to study the parotid glands, showing that the mean gray level and standard deviation (SD) of intensity levels differ significantly between

Address for correspondence: Dr. Li-Jen Liao, Department of Otolaryngology Head and Neck Surgery, Far Eastern Memorial Hospital, No. 21, Sec. 2, Nanya S. Road, Banqiao Dist., New Taipei City 220, Taiwan.
E-mail: deniro@mail2000.com.tw

Received: 26-06-2022 Revised: 26-07-2022 Accepted: 09-08-2022 Available Online: 24-01-2023

Access this article online

Quick Response Code:



Website:
<https://journals.lww.com/jmut>

DOI:
10.4103/jmu.jmu_65_22

This is an open access journal, and articles are distributed under the terms of the Creative Commons Attribution-NonCommercial-ShareAlike 4.0 License, which allows others to remix, tweak, and build upon the work non-commercially, as long as appropriate credit is given and the new creations are licensed under the identical terms.

For reprints contact: WKHLRPMedknow_reprints@wolterskluwer.com

How to cite this article: Lo WC, Cheng PC, Hsu WL, Cheng PW, Liao LJ. A novel prediction model based on quantitative texture analysis of sonographic images for malignant major salivary glandular tumors. *J Med Ultrasound* 2023;31:218-22.

benign and malignant parotid tumors.^[5] Furthermore, the most frequently cited second-order texture analysis method is based on extracting various texture features from a gray level cooccurrence matrix (GLCM) developed by Haralick (1973).^[6]

US-texture analysis in radiation-induced parotid gland injury exhibits significant differences in some sonographic texture features between normal and postradiotherapy glands.^[7] For salivary gland tumors, two features (contrast and entropy) are reported to be significantly different between benign and malignant tumors.^[8] However, the sample size of previous studies was small,^[5,8] and no study has used these objective US characteristics in combination to differentiate malignant from benign salivary gland tumors. The aim of this study was to compare multiple objective US texture features and to develop an objective predictive model for distinguishing malignant major salivary gland tumors.

MATERIALS AND METHODS

This study was approved by the Institutional Ethics Review Board (107186-E) of a tertiary referral center, informed consent was waived by the IRB. From August 2007 to May 2018, 144 consecutive adult patients who had major salivary gland tumors and underwent surgery with definite pathological results were recruited. The sonograms were performed by the corresponding author and first author (both have experience with more than 10,000 US procedures) using a Philips HDI 3500 (Bothell, WA) or Toshiba Aplio MX or 500 (Otagawa, Japan) platform with a high-resolution 5–14-MHz real-time linear-array transducers. A representative brightness mode US picture of each salivary gland tumor was selected for further texture analysis [Figure 1]. Further texture image analysis was performed with ImageJ software (National Institutes of Health, Bethesda, Maryland, USA).

First-order histogram: Intensity analysis in gray level^[4,5]

The gray level of the selected area was measured, and then, we calculated the mean and SD of the gray level.

Second-order Texture analysis with gray level cooccurrence matrix^[6,7,9]

This method was developed by Haralick (1973).^[6] The calculation of various texture characteristics was described in detail in previous literature.^[7-10] We used ImageJ software to estimate the angular second moment (ASM, Energy), contrast, correlation, inverse difference (INV) moment (IDM), dissimilarity, INV, variance, entropy, cluster shade (CS), and cluster prominence (CP). ASM and inverse IDM represent homogeneity; contrast and variance represent heterogeneity; correlation represents smoothness; entropy represents randomness; and CS and CP represent uniformity.

Statistical analysis

Categorical data are expressed as numbers and percentages and continuous data as the mean \pm SD or median (interquartile range), when appropriate. Receiver operating characteristic (ROC) curves were used to find the optimal cutoff points of significant variables.^[11] We used logistic regression models to assess the odds ratios of these variables, and then, stepwise selection ($P = 0.1$) of these factors was performed to develop a predictive model that was constructed with selected predictive variables multiplied by

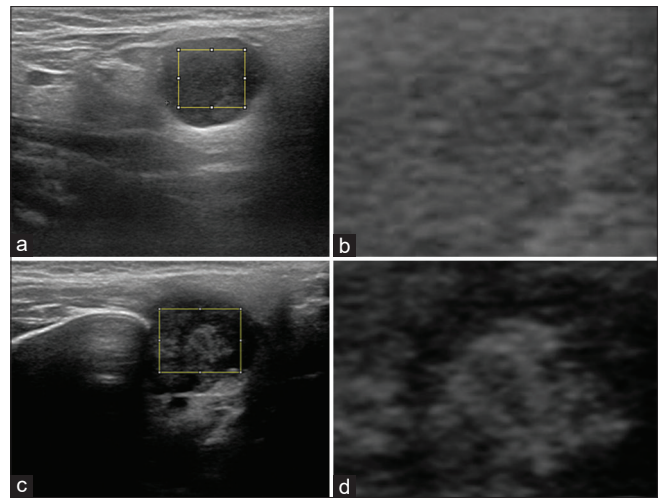


Figure 1: A square block was sampled from a patient with a right parotid tumor (a). A representative US picture was selected for further texture analysis (b). The pathologic report revealed pleomorphic adenoma. Another square block was sampled from a patient with a right parotid tumor with a diagnosis of mucoepidermoid carcinoma (c). Another representative US picture was selected for further texture analysis (d). US: Ultrasound

regression coefficients. The diagnostic performance of this model was analyzed using ROC curve analysis. All statistical analyses were carried out using Stata software, version 12.0 (Stata Corp. LP, College Station, TX, USA).

RESULTS

There were 144 adult patients, 87 males and 57 females, recruited for this study, with a mean age of 53.4 ± 15.2 years old. The detailed demographic characteristics are displayed in Table 1. The final pathology revealed 66 malignancies (16 poorly differentiated carcinomas, 10 squamous cell carcinomas, 8 metastatic carcinomas, 7 adenoid cystic carcinomas, 6 B cell lymphomas, 5 mucoepidermoid carcinomas, 5 invasive carcinomas, 3 lymphoepithelial carcinomas, 3 acinic cell carcinomas, 2 salivary ductal carcinomas, and 1 adenocarcinoma) and 78 benign lesions (32 pleomorphic adenomas, 23 Warthin's tumors and 23 other benign lesions (4 basal cell adenomas, 4 chronic inflammatory lesions, 3 lymphoepithelial cysts, 3 chronic sclerosing sialadenitis, 2 benign cysts, 2 nodular fasciitis, 1 lipoma, 1 mucocoele, 1 epidermal cyst, 1 reactive hyperplasia, and 1 oncocytic neoplasm). The mean age of the patients who had malignant tumors was greater than that of those who had benign tumors ($P < 0.05$).

The grayscale intensity and SD results are displayed in Figure 2. We found that the intensity of pleomorphic adenoma was significantly higher than that of malignant tumors [Figure 2a]. However, the intensity of malignant tumors was not different from Warthin's tumor or other benign tumors. In addition, the SD of malignant tumors was higher than that of pleomorphic adenomas [Figure 2b].

The results of the GLCM texture analysis are shown in Table 2. Multiple variables (including contrast, IDM, entropy, dissimilarity, and INV) were significantly different between malignancy and benignity. Table 3 shows the odds ratios of these

Table 1: Demographic data for the recruited patients

Variables	Malignant (n=66; 47%), n (%)	Benign (n=78; 53%), n (%)	Total (n=144; 100%), n (%)	P
Sex				
Male	40 (46)	47 (54)	87 (60)	0.9662
Female	26 (46)	31 (54)	57 (40)	
Age (years)	56.55±17.34 (21-93)	50.77±12.64 (22-89)	53.42±15.20 (21-93)	0.0225*
Site				
Parotid	43 (39)	67 (61)	110 (76)	0.003*
SM	23 (68)	11 (32)	34 (24)	
Size (cm)				
Short axis	2.08±2.38 (1.50-2.66)	1.57±0.60 (1.44-1.71)	1.80±1.68 (1.53-2.08)	0.0708
Long axis	2.56±0.98 (2.32-2.80)	2.35±0.99 (2.13-2.58)	2.45±0.99 (2.29-2.61)	0.2146
Alcohol drinking	14 (47)	16 (53)	30 (22)	0.3232
Smoking	19 (38)	31 (62)	50 (36)	0.1963
Betel nut chewing	9 (41)	13 (59)	22 (16)	0.6531
Pathology				
Poorly differentiated carcinomas		16		
Squamous cell carcinomas		10		
Metastatic carcinomas		8		
Adenoid cystic carcinomas		7		
B-cell lymphomas		6		
Mucoepidermoid carcinomas		5		
Invasive carcinomas		5		
Lymphoepithelial carcinomas		3		
Acinic cell carcinomas		3		
Salivary ductal carcinomas		2		
Adenocarcinomas		1		
Pleomorphic adenomas		32		
Warthin's tumors		23		
Basal cell adenomas		4		
Chronic inflammation cases		4		
Lymphoepithelial cysts		3		
Chronic sclerosing sialadenitis cases		3		
Benign cysts		2		
Nodular fasciitis cases		2		
Lipoma		1		
Mucocele		1		
Epidermal cyst		1		
Reactive hyperplasia		1		

SM: Submandibular, *P <0.05

variables with the optimal cutoff level for predicting malignancy. We dichotomized the odds ratio according to the optimal cutoff, which was determined at the point of highest accuracy for predicting malignancy by ROC curve analysis. As a result, the optimal cutoff odds values of age (≥ 60), intensity (≥ 51.39), contrast (≥ 7.15), IDM (≥ 3.36), dissimilarity (≥ 7.12), and INV (≥ 0.41) were 3.3 (95% confidence interval [CI]: 1.6–6.7), 0.2 (0.1–0.5), 7.1 (3.4–15.0), 0.3 (0.1–0.5), 5.7 (2.6–12.8), 10.1 (3.6–28.3), and 0.3 (0.1–0.5), respectively. Multivariate stepwise logistic regression analysis was further performed to identify four independent factors (including age, intensity, contrast, and entropy) predicting malignant major salivary gland tumors. These four parameters were applied to develop an objective model for the prediction of malignant salivary gland tumors. The predictive model was as follows: $1.138 \times \text{Age} - 1.814 \times \text{Intensity}$

$+ 1.416 \times \text{Entropy} + 1.714 \times \text{Contrast}$. With the optimal cutoff value of 0.58, the diagnostic performance of this model showed a sensitivity of 83%, specificity of 74%, and overall accuracy of 78% [Table 4 and Figure 3].

DISCUSSION

This is the first study to propose a prediction model based on objective US texture characteristics to predict malignant major salivary gland tumors. An objective sonographic predictive model may be feasible to diagnose malignant major salivary glandular tumors and waive the necessity of subjective judgment.

Subjective US characteristics for malignant salivary gland tumors include irregular shape, unclear boundary, the absence of posterior acoustic enhancement, heterogeneous internal echo,

Table 2: Comparisons of second-order texture characteristics between malignant and benign salivary glandular tumors (mean±standard deviation)

Features	Subject	ASM (×10 ⁴)	Contrast (×10 ⁻²)	Correlation (×10 ⁴)	IDM (×10 ²)	Entropy	Dissimilarity	INV	Variance (×10 ⁻²)	CS (×10 ⁻⁴)	CP (×10 ⁻⁶)
0°	Malignant (n=66)	0.83±2.12	5.43±5.10	2.73±1.94	4.66±2.38	6.44±1.06	2.88±2.43	0.52±0.20	11.09±8.26	6.47±1.24	2.50±3.92
	Benign (n=78)	1.40±4.07	2.16±2.18	3.35±2.12	6.23±1.66	5.79±0.71	1.30±0.90	0.65±0.14	8.67±6.43	3.96±1.19	1.46±2.91
	P	0.3063	0.0000*	0.0736	0.0000*	0.0000*	0.0000*	0.0000*	0.0509	0.2176	0.0700
45°	Malignant (n=66)	0.60±1.86	14.54±14.01	2.41±1.76	3.09±1.87	7.04±1.03	5.70±4.35	0.38±0.17	11.33±8.35	5.87±1.19	2.37±3.76
	Benign (n=78)	1.07±3.73	6.02±5.89	2.95±1.91	4.22±1.49	6.46±0.78	2.91±2.01	0.48±0.13	8.88±6.38	3.75±1.17	1.44±2.80
	P	0.3543	0.0000*	0.0821	0.0001*	0.0002*	0.0000*	0.0000*	0.0580	0.2841	0.0938
90°	Malignant (n=66)	0.66±2.00	11.33±9.86	2.55±1.83	3.36±2.00	6.93±1.04	4.90±3.74	0.40±0.18	11.13±8.24	6.09±1.20	2.37±3.78
	Benign (n=78)	1.13±3.80	3.99±4.15	3.22±2.04	4.58±1.60	6.35±0.79	2.46±1.77	0.51±0.14	8.72±6.41	3.85±1.17	1.43±2.82
	P	0.3615	0.0000*	0.0529	0.0001*	0.0002*	0.0000*	0.0000*	0.0514	0.2537	0.0902
135°	Malignant (n=66)	0.60±1.85	15.12±14.52	2.38±1.75	3.08±1.87	7.04±1.03	5.74±4.38	0.38±0.17	11.32±8.32	5.92±1.18	2.35±3.71
	Benign (n=78)	1.06±3.70	6.02±5.76	2.91±1.87	4.22±1.50	6.47±0.78	2.93±2.02	0.48±0.13	8.88±6.37	3.75±1.17	1.44±2.81
	P	0.3547	0.0000*	0.0816	0.0001*	0.0002*	0.0000*	0.0000*	0.0580	0.2717	0.0973
Average	Malignant (n=66)	0.65±1.96	11.79±10.57	2.54±1.84	3.35±2.03	6.98±1.09	4.80±3.70	0.42±0.18	11.22±8.29	6.09±1.20	2.40±2.83
	Benign (n=78)	1.15±3.82	4.54±4.41	3.09±1.95	4.82±1.55	6.34±0.79	2.40±1.67	0.53±0.13	8.79±6.40	3.83±1.18	1.44±2.83
	P	0.3399	0.0000*	0.0838	0.0000*	0.0001*	0.0000*	0.0000*	0.0595	0.2565	0.0869

*Indicates a significant difference. ASM: Angular second moment, IDM: Inverse difference moment, INV: Inverse difference, CS: Cluster shade, CP: Cluster prominence

Table 3: Univariate logistic regression analyses of clinical and subjective texture factors for malignant major salivary gland tumors

Items	Odds ratio	95% CI		P
Age (years) (≥60)	3.299	1.626	6.693	0.001*
Intensity (≥51.39)	0.229	0.110	0.475	0.000*
Contrast (×10 ⁻²) (≥7.1491)	7.142	3.419	14.922	0.000*
IDM (×10 ²) (≥3.36)	0.268	0.132	0.545	0.000*
Entropy (≥7.119)	5.732	2.576	12.755	0.000*
Dissimilarity (≥5.224)	10.108	3.607	28.323	0.000*
INV (≥0.414)	0.250	0.122	0.511	0.000*

IDM: Inverse difference moment, INV: Inverse difference, CI: Confidence interval, *P<0.05

and calcification.^[3,12-15] However, there is still a reliance on human expertise. Therefore, we sought to adapt texture analysis to develop an objective prediction model. In first-order texture analysis, we found that the intensity and SD of intensity were significantly different between malignant major salivary gland tumors and pleomorphic adenomas. Malignant and Warthin's tumors are relatively hypointense and have a higher SD of intensity than pleomorphic adenomas. In serial comparisons, the difference was most prominent between malignant tumors and pleomorphic adenomas [Figure 2]. These findings are comparable with our clinical observation that malignant and Warthin's tumors are relatively more hypoechoic and have a more heterogeneous echo pattern than pleomorphic adenomas.

In second-order texture analysis, we also found that several texture features, including contrast, IDM, entropy, dissimilarity, and INV, differed significantly between benign and malignant major salivary gland tumors. These characteristics are relatively difficult to judge quantitatively and subjectively. Our findings reveal that malignancy shows higher contrast, entropy, and dissimilarity but lower IDM and INV. These findings are also comparable with those of a previous publication.^[8]

We then performed multivariate stepwise logistic regression analysis to identify four independent factors and further developed an objective predictive model, namely, 1.138×Age-1.814×Intensity+1.416×Entropy+1.714×Contrast, that predicts malignant major salivary gland tumors. The best cutoff for predicting malignant major salivary gland tumors was ≥0.58, corresponding to a sensitivity of 83% (74%-92%), specificity of 74% (65%-84%), overall accuracy of 78% (65%-84%), and area under the curve of 0.86 (0.80-0.92).

This study has some limitations. The pathology of salivary gland cancer is heterogeneous, and this was a single-institution retrospective study. We only analyzed objective characteristics (image texture) of tumors, and some subjective US features that are reported to be associated with malignancy, such as posterior acoustic enhancement, boundary, and shape, were not included. Although we collect numerous features, the result of this subjective prediction model is still not superior to our previous model based on professional ultrasonologist's judgment.^[3] Further large-scale studies that

Table 4: Performance of the objective predictive scoring model

Items	Sensitivity (95% CI)	Specificity (95% CI)	Overall accuracy (95% CI)	AUC	95% CI
Model (≥ 0.58)	83.33% (74.34-92.32)	74.36% (64.67-84.05)	78.47% (71.76-85.19)	0.86	0.80-0.92

Model = $1.138 \times \text{Age} - 1.814 \times \text{Intensity} + 1.416 \times \text{Entropy} + 1.714 \times \text{Contrast}$. CI: Confidence interval, AUC: Area under the curve

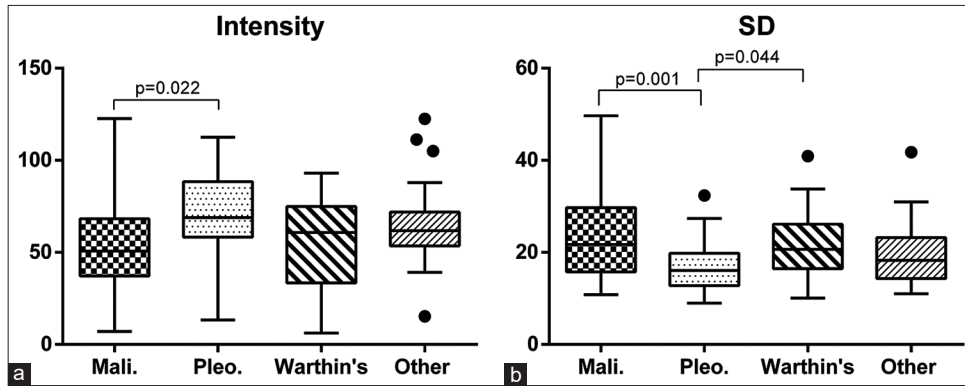


Figure 2: Comparisons of intensity (a) and SD of intensity (b) between malignant and benign tumors. SD: Standard deviation, Mali.: Malignant, Pleo.: Pleomorphic adenoma

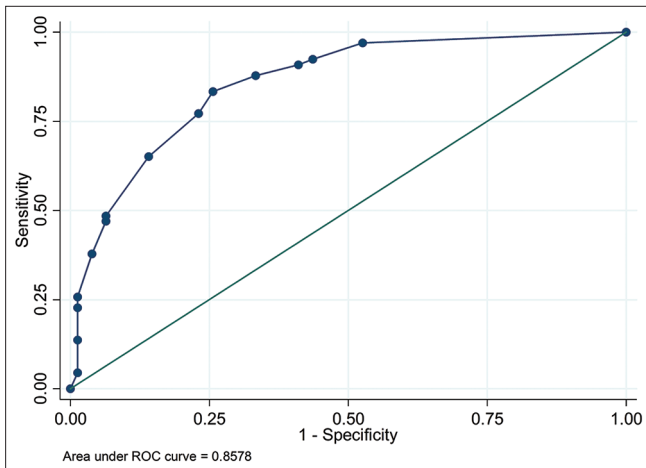


Figure 3: ROC analysis of the objective prediction model (AUC = 0.86). ROC: Receiver operating curve, AUC: Area under the curve

incorporate these characteristics to adjust and advance this predictive model are necessary.

CONCLUSION

We have developed a novel computerized diagnostic model based on objective US features to predict malignant major salivary gland tumor. Further improving the computer-aided diagnosis model might change the US examination for major salivary gland tumor in the future.

Financial support and sponsorship

This work is supported by a grant from the Far Eastern Memorial Hospital Research Program (FEMH-2022-C-70). This funding source had no role in the design of this study or in its execution, analyses, interpretation of the data, or decision to submit the results.

Conflicts of interest

There are no conflicts of interest.

REFERENCES

- Cheng PC, Chang CM, Huang CC, Lo WC, Huang TW, Cheng PW, et al. The diagnostic performance of ultrasonography and computerized tomography in differentiating superficial from deep lobe parotid tumours. *Clin Otolaryngol* 2019;44:286-92.
- Katz P, Hartl DM, Guerre A. Clinical ultrasound of the salivary glands. *Otolaryngol Clin North Am* 2009;42:973-1000.
- Lo WC, Chang CM, Wang CT, Cheng PW, Liao LJ. A novel sonographic scoring model in the prediction of major salivary gland tumors. *Laryngoscope* 2021;131:E157-62.
- Martins de Almeida M. Use of statistical techniques to analyze textures in medical images for tumor detection and evaluation. *Adv Mol Imaging Interv Radiol* 2018;1:01-6.
- Yonetsu K, Ohki M, Kumazawa S, Eida S, Sumi M, Nakamura T. Parotid tumors: Differentiation of benign and malignant tumors with quantitative sonographic analyses. *Ultrasound Med Biol* 2004;30:567-74.
- Haralick RM, Shanmugam K, Dinstein IH. Textural features for image classification. *IEEE Trans Syst Man Cybern* 1973;SMC-3:610-21.
- Yang X, Tridandapani S, Beitler JJ, Yu DS, Yoshida EJ, Curran WJ, et al. Ultrasound GLCM texture analysis of radiation-induced parotid-gland injury in head-and neck cancer radiotherapy: An *in vivo* study of late toxicity. *Med Phys* 2012;39:5732-9.
- Chikui T, Tokumori K, Yoshiura K, Oobu K, Nakamura S, Nakamura K. Sonographic texture characterization of salivary gland tumors by fractal analyses. *Ultrasound Med Biol* 2005;31:1297-304.
- Bhatia KS, Lam AC, Pang SW, Wang D, Ahuja AT. Feasibility study of texture analysis using ultrasound shear wave elastography to predict malignancy in thyroid nodules. *Ultrasound Med Biol* 2016;42:1671-80.
- Prakash MJ, Kezia S, Prabha IS, Kumar VV. A new approach for texture segmentation using gray level textons. *Int J Signal Process, Image Process Pattern Recognit* 2013;6:81-90.
- Yin J, Tian L. Joint confidence region estimation for area under ROC curve and Youden index. *Stat Med* 2014;33:985-1000.
- Abdel Razek AA, Mukherji SK. State-of-the-art imaging of salivary gland tumors. *Neuroimaging Clin N Am* 2018;28:303-17.
- Bialek EJ, Jakubowski W, Karpińska G. Role of ultrasonography in diagnosis and differentiation of pleomorphic adenomas: Work in progress. *Arch Otolaryngol Head Neck Surg* 2003;129:929-33.
- Schick S, Steiner E, Gahleitner A, Böhm P, Helbich T, Ba-Ssalamah A, et al. Differentiation of benign and malignant tumors of the parotid gland: Value of pulsed Doppler and color Doppler sonography. *Eur Radiol* 1998;8:1462-7.
- Kim J, Kim EK, Park CS, Choi YS, Kim YH, Choi EC. Characteristic sonographic findings of Warthin's tumor in the parotid gland. *J Clin Ultrasound* 2004;32:78-81.